

Sideband cooling an ion to the quantum ground state in a Penning trap with very low heating rate

J.F. Goodwin, G. Stutter, R.C. Thompson, and D.M. Segal
*Quantum Optics and Laser Science, Blackett Laboratory, Imperial College London,
Prince Consort Road, London, SW7 2AZ, United Kingdom.*

We report the laser cooling of a single $^{40}\text{Ca}^+$ ion in a Penning trap to the motional ground state in one dimension. Cooling is performed in the strong binding limit on the 729-nm electric quadrupole $S_{1/2} \leftrightarrow D_{5/2}$ transition, broadened by a quench laser coupling the $D_{5/2}$ and $P_{3/2}$ levels. We find the final phonon number to be $\bar{n} = 0.012 \pm 0.009$. We measure the heating rate of the trap to be exceptionally low with $\dot{n} = 0.08 \pm 0.12 \text{ s}^{-1}$ and a scaled spectral noise density of $\omega S_\omega < 1.6 \times 10^{-10} \text{ V}^2 \text{ m}^{-2} \text{ Hz}^{-1} \text{ s}^{-1}$, which is consistent with the large ion-electrode distance. We perform Rabi oscillations on the sideband-cooled ion and observe a coherence time of $0.7 \pm 0.1 \text{ ms}$, noting that the practical performance is limited primarily by the intensity noise of the probe laser.

Cold, trapped ions are one of the leading systems with which to study quantum processes that require excellent environmental isolation, including quantum computation [1], quantum simulation [2], frequency standards [3] and measurements of fundamental constants [4].

Penning traps [5, 6] provide an alternative to the more common radiofrequency (RF) trap and offer an excellent degree of precision and isolation. Penning traps can achieve reasonable trapping frequencies at large ($\sim 1 \text{ cm}$) electrode distances, reducing the ion heating rate and other environmental noise; they provide near-perfect frequency-selective state preparation and readout due to the large Zeeman splitting; and they can be used without any oscillating fields, making them suitable for trapping 2- and 3-D Coulomb crystals [7] and ions in delicate states that can be perturbed by RF fields (e.g. Rydberg ions [8]). These types of experiment often require the ion to be confined to the motional ground state, which is generally achieved via resolved sideband cooling. The sideband cooling technique was perfected in RF traps many years ago [9, 10], but due to the increased technical complexities associated with the Penning trap, it has yet to be realised in this system.

In this Letter we demonstrate the application of resolved sideband cooling to the Penning trap, cooling the axial motion of a single calcium ion to its quantum ground state with 99% probability. We measure the heating rate of the trap, which we find to be the lowest yet reported, by over an order of magnitude. The low heating rate is consistent with the large dimensions of the trap, which has a characteristic dimension of $d_0 = 1.32 \text{ cm}$, with the distance to the nearest electrode $d = 1.08 \text{ cm}$. Finally, we demonstrate the coherence of our cooled ion by observing its Rabi dynamics.

We recently reported work on resolved sideband spectroscopy and thermometry of a single ion in a Penning trap [11] and the experiments described here use a modified version of the same apparatus. We trap a single $^{40}\text{Ca}^+$ ion in a Penning trap consisting of a stack of concentric cylindrical electrodes, held in a 1.84 T axial field

provided by a superconducting solenoid magnet. Doppler cooling in the axial and radial directions is performed on the 397-nm dipole-allowed $S_{1/2} \leftrightarrow P_{1/2}$ transition, with a set of four laser frequencies around 866 nm applied along the trap axis to repump population trapped in the metastable $D_{3/2}$ states. At high magnetic fields, j -state mixing [12] provides a small but significant branching ratio of $4.2 \times 10^{-7} B^2/T^2$ to the $D_{5/2}$ manifold, and a further set of four laser frequencies around 854 nm are required to prevent population trapping in these states. A laser at 729 nm, addressing the electric quadrupole $S_{1/2} \leftrightarrow D_{5/2}$ transition, is used for resolved sideband spectroscopy via the electron shelving technique. Details of the trap geometry, Doppler cooling laser systems and spectroscopy scheme can be found in [11] and [13].

We have made two major changes to the experiment to enable us to perform sideband cooling. The first is an increase in the power of the 729-nm laser through use of a tapered amplifier. This increases the power at the ion from approximately 4 mW to 40 mW, allowing us to reach high enough Rabi frequencies ($\Omega_0 \sim 2\pi \times 50 \text{ kHz}$) to sideband cool on this transition. We do not require this boost to increase the resonant absorption rate, but to ensure that the cooling remains robust against small frequency drifts of several kHz during the course of the experiment, which are due to mechanical instabilities of the trap within the magnetic field. The effective width of spectral features increases with the Rabi frequency, making small detunings from the centre of the feature less significant.

The second change is to introduce a weak, oscillating quadrupolar ‘axialisation’ field [14] to couple the magnetron and modified cyclotron radial trap modes. The work in the previous paper [11] was performed without any oscillating fields, using an intensity gradient across the radial cooling beam to cool the otherwise-unstable magnetron motion [15]. However, for higher axial frequencies, the required radial intensity gradient increases, and with our current optical system we were unable to reliably cool ions above axial frequencies of $\sim 200 \text{ kHz}$.

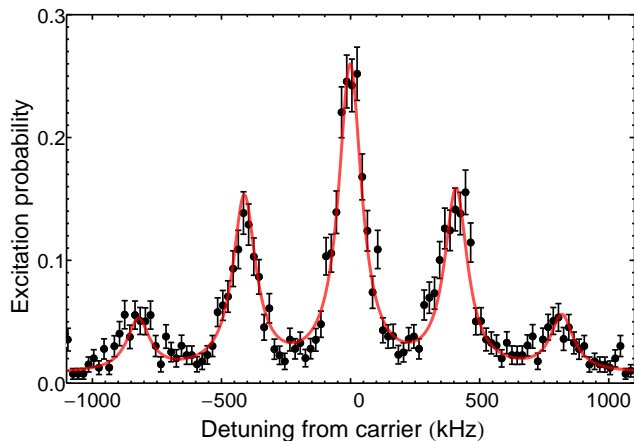


FIG. 1: Typical axial motional sideband spectrum after Doppler cooling. The solid line is a fit to a comb of Lorentzians with heights driven by the Rabi dynamics of a thermally distributed population, giving $\bar{n} = 26 \pm 2$, equivalent to a temperature of 0.51 ± 0.04 mK.

The axialisation technique, which had been used by the group in earlier experiments [16, 17], works at all trap frequencies, but had previously been limited by a small misalignment of the axialisation field with respect to the DC trapping potential. Having rectified this through the use of a more versatile axialisation drive supply we can now efficiently cool at all axial frequencies up to the stability limit of the trap, and achieve much lower phonon numbers after Doppler cooling.

The ion is initially Doppler cooled, before one of the two 397-nm lasers is switched off to optically pump population into the $S_{1/2}(m_j = +\frac{1}{2})$ sub-level. Sideband cooling is performed by applying the 729-nm laser to the first red axial sideband of the $S_{1/2}(m_j = +\frac{1}{2}) \leftrightarrow D_{5/2}(m_j = -\frac{1}{2})$ transition, while using a weak 854-nm quench laser to increase the scattering rate by emptying the $D_{5/2}$ level via $P_{3/2}$. Provided the saturation parameter of the quench laser is small, the $P_{3/2}$ level can be adiabatically eliminated and the system behaves like a virtual two level system with a controllable linewidth set by the properties of the quench laser and upper level [18]. The second 397-nm laser and 866-nm repump lasers are applied throughout the sequence to ensure that population decaying on the $P_{3/2} \leftrightarrow S_{1/2}$ transition is optically pumped into the correct ($m_j = +\frac{1}{2}$) ground state sub-level. After sideband cooling, electron shelving spectroscopy is performed as described in [11].

RESULTS

The ion is trapped with an axial frequency of 405 kHz and Doppler cooled for 5 ms. We measure an axial temperature of 0.51 mK, 1.33 times the Doppler cool-

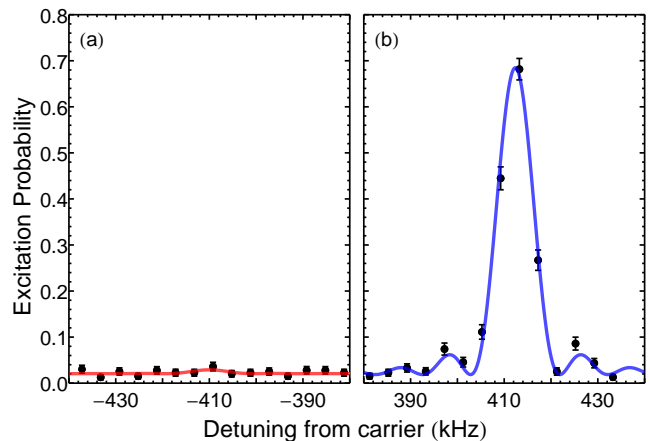


FIG. 2: (a) First red and (b) first blue sidebands after 21 ms of cooling on the first red sideband. The ratio of the sideband heights above the background shows that the average phonon number is $\bar{n} = 0.012 \pm 0.009$.

ing limit, corresponding to an average phonon number of $\bar{n} = 26 \pm 2$. Figure 1 shows a typical axial sideband spectrum after this step. We do not measure a radial temperature directly during these experiments, but previous work suggests this is several times higher than the axial temperature [11]. Note that for this trap frequency, the 729-nm axial Lamb-Dicke parameter is $\eta_{729} = 0.15$ and the ion remains somewhat outside the Lamb-Dicke regime ($\eta_{729}^2(2\bar{n}+1) \sim 1.2$) after Doppler cooling, though not far enough to prevent us from cooling efficiently on the first red sideband.

Figure 2 shows the first red and blue sidebands after 21 ms of sideband cooling. The blue sideband is fitted to a Rabi-Lorentzian profile on a constant background. Because the blue sideband Rabi dynamics in $n = 0$ are identical to the red sideband dynamics in $n = 1$, and $\bar{n} \ll 1$, the red sideband is correctly described by the sum of a uniform background and the blue profile scaled by \bar{n} . The fit shows the average phonon number after sideband cooling to be $\bar{n} = 0.012 \pm 0.009$.

The heating rate of the trap is measured by cooling to the ground state and inserting a delay period before spectroscopy is performed, during which no cooling is applied. The change in the ratio of the red and blue sideband heights then allows the change in phonon number during this delay to be determined.

We perform two heating rate measurements, with delays of 100 ms and 200 ms, at an axial trap frequency of 405 kHz. We observe almost no heating after either delay, the results of which are summarised in Figure 3. A measurement at a longer delay time, where a more significant red sideband might be observed, would help constrain this fit. However, due to slow drifts in the frequency of the transition caused by thermal movement of the trap vacuum chamber within the magnet bore, we are currently unable to keep the sideband cooling sequence per-

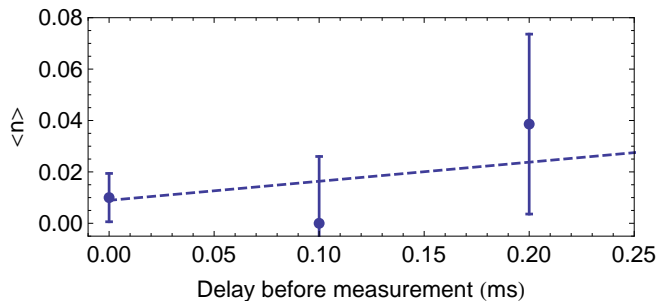


FIG. 3: The heating rate is determined by measuring the phonon number after a variable delay between cooling and spectroscopy. The fitted line gives a heating rate of $\dot{n} = 0.07 \pm 0.12 \text{ s}^{-1}$.

forming correctly without any adjustment for the many hours necessary to produce the required spectrum. Nevertheless, although the uncertainties on these values are very large, the heating rate of $\dot{n} = 0.07 \pm 0.12 \text{ s}^{-1}$ is extremely low, as would be expected from such a large trap.

In Figure 4 we compare our trap heating rate to those of a variety of other traps, plotted against the distance to the nearest electrode. Here we have taken the usual approach of plotting the phonon heating rate in terms of an inferred noise spectral density, $\omega S_E(\omega) = 4m\hbar\omega\dot{n}/e^2$, scaled by the trap frequency ω . Note that we have not included any cryogenically cooled traps, nor those that have undergone any in-situ surface treatment. For ease of comparison, we have also only considered traps with 3-dimensional electrode structures. Our heating rate, shown in the lower right corner, is an order of magnitude lower than any other ion trap reported to date, including those we have excluded from this plot.

There has been a great deal of research over the last decade into the underlying mechanism of heating in ion traps, and in particular the heating due to the proximity of electrode surfaces [19]. A discussion of this topic is beyond the scope of this letter. It suffices to say that it has become increasingly apparent in recent years that the dominant heating mechanism varies between traps and that this behaviour cannot necessarily be encapsulated in a single power-law, such as the oft-quoted $1/d^4$ electrode distance scaling [20]. With this proviso, we nonetheless provide a power law fit to the data shown in Figure 4 for approximate reference only, giving a $1/d^{3.1}$ dependence.

We now present some basic demonstrations of the coherence of our qubit and probe laser. We probe the ion on the carrier transition and observe Rabi oscillations after Doppler cooling only (Figure 5(a)) and after sideband cooling to the motional ground state (Figure 5(b)). After Doppler cooling, the ion is in an approximately thermal distribution with $\bar{n} = 35 \pm 5$, determined by fitting to a full spectrum as in Figure 1. The Rabi oscillations rapidly lose contrast due to the large number of con-

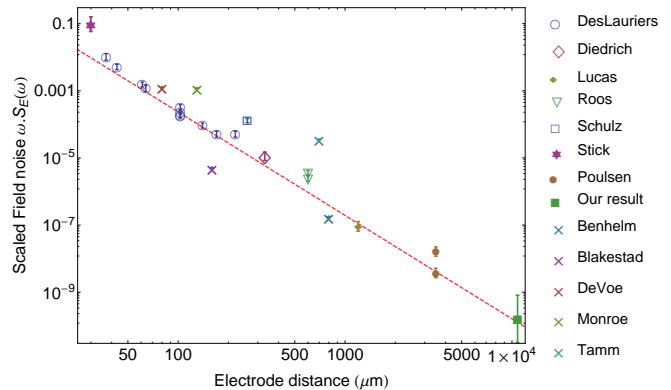


FIG. 4: The reported heating rates of a variety of linear, ring and needle traps, shown as a frequency-scaled, noise spectral density plotted against the distance to the nearest electrode. The result reported in this Letter is shown in the lower right corner. The solid line is a fit to a $1/d^\alpha$ power law dependence, giving $\alpha = 3.1 \pm 0.2$. No uncertainty data is available for the results marked with “X” and these do not contribute to the fit. [Data sources: DesLauriers [21], Diedrich [9], Roos [10], Schulz [22], Stick [23], Poulsen [24], Benhelm [25], Blakestad [26], DeVoe [27], Monroe [28], Tamm [29]]

tributing frequencies, and the corresponding fit provides an independent measure of $\bar{n} = 31 \pm 2$.

After ground state cooling, with $\bar{n} \sim 0.01$, the Rabi oscillations are well defined, with a coherence time of $\tau = 0.7 \pm 0.1 \text{ ms}$, approximately consistent with our spectroscopically measured linewidth of $\Delta\nu = 0.6 \pm 0.4 \text{ kHz}$ [11]. Note that the fit to the first half of the data gives a Rabi frequency of $\Omega_0 = 2\pi \times 41 \text{ kHz}$ and the second half $\Omega_0 = 2\pi \times 39 \text{ kHz}$, with a noisy discontinuity between the two. This is due to uncontrolled intensity noise on

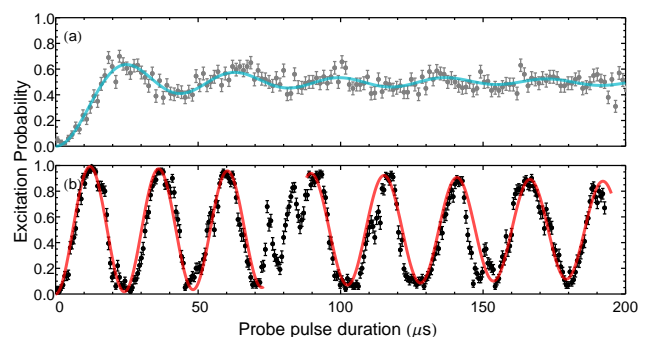


FIG. 5: (a) Rabi oscillation on the carrier after Doppler cooling. The fit is to the summed Rabi dynamics of a thermal distribution of Fock states and gives $\Omega_0 \sim 2\pi \times 27 \text{ kHz}$. The oscillations rapidly lose contrast as $\bar{n} \sim 30$. (b) Rabi oscillation on the carrier after ground state cooling. The Rabi frequency is initially $\Omega_0 \sim 2\pi \times 41 \text{ kHz}$ but laser intensity noise causes an abrupt shift at $70 \mu\text{s}$ and the fit to the remainder of the plot gives $\Omega_0 \sim 2\pi \times 39 \text{ kHz}$. The overall visibility decays exponentially with a coherence time of $\tau = 0.7 \pm 0.1 \text{ ms}$.

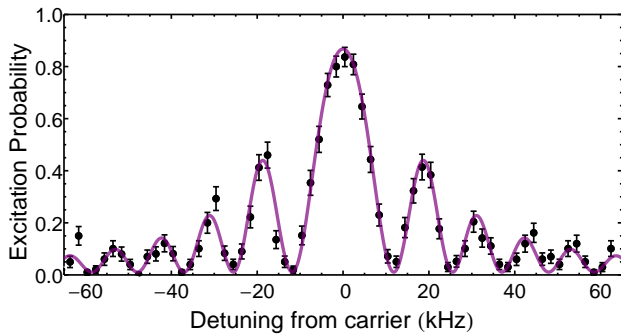


FIG. 6: High-resolution scan of the Rabi dynamics of a 100 μ s probe pulse on the carrier after sideband cooling to the ground-state. The solid line is a fit to the theory from which we deduce a pulse area on resonance of 3.25π

the 729-nm probe laser, whose intensity is boosted by an injection locked slave laser followed by a tapered amplifier and is thus affected by mechanical drifts in these systems. We are currently developing an intensity-noise-eating feedback system for this laser and are also improving the beam pointing stability into the trap.

Figure 6 shows the Rabi dynamics as the probe laser is detuned from the carrier transition. The probe time is 100 μ s and the Rabi-Lorentzian fit gives a pulse area on resonance of 3.25π .

We have demonstrated the application of resolved sideband laser cooling to an ion in a Penning trap, achieving occupancy of the quantum ground state with 99% probability. We have measured the heating rate of our ion trap and found it to be exceptionally low. We believe these results provide compelling evidence that Penning trapped ions are an excellent choice of system for a range of precision experiments in quantum information [30], quantum thermodynamics [31] and fundamental measurement [32].

-
- [1] D. Nigg, M. Müller, E. A. Martinez, P. Schindler, M. Hennrich, T. Monz, M. A. Martin-Delgado, and R. Blatt, *Science* **345**, 302 (2014).
- [2] J. W. Britton, B. C. Sawyer, A. C. Keith, C. C. J. Wang, J. K. Freericks, H. Uys, M. J. Biercuk, and J. J. Bollinger, *Nature* **484**, 489 (2012).
- [3] P. Gill, G. P. Barwood, H. A. Klein, G. Huang, S. A. Webster, P. J. Blythe, K. Hosaka, S. N. Lea, and H. S. Margolis, *Measurement Science and Technology* **14**, 1174 (2003).
- [4] W. Quint, J. Dilling, S. Djekic, H. Häffner, N. Hermanspahn, H.-J. Kluge, G. Marx, R. Moore, D. Rodriguez, J. Schnfelder, et al., *Hyperfine Interactions* **132**, 453 (2001).
- [5] R. C. Thompson, S. Donnellan, D. R. Crick, and D. M. Segal, *Journal of Physics B: Atomic, Molecular and Optical Physics* **42**, 154003 (2009).
- [6] L. S. Brown and G. Gabrielse, *Rev. Mod. Phys.* **58**, 233 (1986).
- [7] S. Mavadia, J. Goodwin, G. Stutter, S. Bharadia, D. Crick, D. Segal, and R. Thompson, *Nat. Comms.* **4**, 2571 (2013).
- [8] M. Müller, L. Liang, I. Lesanovsky, and P. Zoller, *New Journal of Physics* **10**, 093009 (2008).
- [9] F. Diedrich, J. C. Bergquist, W. M. Itano, and D. J. Wineland, *Phys. Rev. Lett.* **62**, 403 (1989).
- [10] C. Roos, T. Zeiger, H. Rohde, H. C. Nägerl, J. Eschner, D. Leibfried, F. Schmidt-Kaler, and R. Blatt, *Phys. Rev. Lett.* **83**, 4713 (1999).
- [11] S. Mavadia, G. Stutter, J. F. Goodwin, D. R. Crick, R. C. Thompson, and D. M. Segal, *Phys. Rev. A* **89**, 032502 (2014).
- [12] D. R. Crick, S. Donnellan, D. M. Segal, and R. C. Thompson, *Phys. Rev. A* **81**, 052503 (2010).
- [13] S. Mavadia, Ph.D. thesis, Imperial College London (2013), URL <http://www3.imperial.ac.uk/iontrap/pubs>.
- [14] R. J. Hendricks, E. S. Phillips, D. M. Segal, and R. C. Thompson, *Journal of Physics B: Atomic, Molecular and Optical Physics* **41**, 035301 (2008).
- [15] W. M. Itano and D. J. Wineland, *Phys. Rev. A* **25**, 35 (1982).
- [16] H. F. Powell, D. M. Segal, and R. C. Thompson, *Phys. Rev. Lett.* **89**, 093003 (2002).
- [17] E. S. Phillips, R. J. Hendricks, A. M. Abdulla, H. Ohadi, D. R. Crick, K. Koo, D. M. Segal, and R. C. Thompson, *Phys. Rev. A* **78**, 032307 (2008).
- [18] I. Marzoli, J. I. Cirac, R. Blatt, and P. Zoller, *Phys. Rev. A* **49**, 2771 (1994).
- [19] D. Hite, Y. Colombe, A. Wilson, D. Allcock, D. Leibfried, D. Wineland, and D. Pappas, *MRS Bulletin* **38**, 826 (2013), ISSN 1938-1425.
- [20] A. Safavi-Naini, P. Rabl, P. F. Weck, and H. R. Sadeghpour, *Phys. Rev. A* **84**, 023412 (2011).
- [21] L. Deslauriers, S. Olmschenk, D. Stick, W. K. Hensinger, J. Sterk, and C. Monroe, *Phys. Rev. Lett.* **97**, 103007 (2006).
- [22] S. A. Schulz, U. Poschinger, F. Ziesel, and F. Schmidt-Kaler, *New Journal of Physics* **10**, 045007 (2008).
- [23] D. Stick, W. K. Hensinger, S. Olmschenk, M. J. Madsen, K. Schwab, and C. Monroe, *Nature Physics* **2**, 39 (2006).
- [24] G. Poulsen, Y. Miroshnychenko, and M. Drewsen, *Phys. Rev. A* **86**, 051402 (2012).
- [25] J. Benhelm, G. Kirchmair, C. F. Roos, and R. Blatt, *Phys. Rev. A* **77**, 062306 (2008).
- [26] R. B. Blakestad, C. Ospelkaus, A. P. VanDevender, J. H. Wesenberg, M. J. Biercuk, D. Leibfried, and D. J. Wineland, *Phys. Rev. A* **84**, 032314 (2011).
- [27] R. G. DeVoe and C. Kurtsiefer, *Phys. Rev. A* **65**, 063407 (2002).
- [28] C. Monroe, D. M. Meekhof, B. E. King, S. R. Jefferts, W. M. Itano, D. J. Wineland, and P. Gould, *Phys. Rev. Lett.* **75**, 4011 (1995).
- [29] C. Tamm, D. Engelke, and V. Bühner, *Phys. Rev. A* **61**, 053405 (2000).
- [30] J. F. Goodwin, B. J. Brown, G. Stutter, H. Dale, R. C. Thompson, and T. Rudolph, arxiv:1407.1858v1 (2014).
- [31] A. Ruiz, D. Alonso, M. B. Plenio, and A. del Campo, *Phys. Rev. B* **89**, 214305 (2014).
- [32] M. Niemann, A.-G. Paschke, T. Dubielzig, M. Carsjens, M. Kohnen, H. Hahn, S. Grondkowski, and C. Ospelkaus, in *IonTech 2* (2013), URL http://www.lkb.ens.fr/iontech2/images/booklet_iontech2.pdf.